

Optimal Aircraft Control Upset Recovery With and Without Component Failures

Dean W. Sparks Daniel D. Moerder

Guidance and Control Branch
NASA Langley Research Center
Hampton, Virginia 23681-2199

1 Introduction

This paper treats the problem of recovering sustainable non-descending (safe) flight in a transport aircraft after one or more of its control effectors fail. Such recovery can be a challenging goal for many transport aircraft currently in the operational fleet for two reasons. First, they have very little redundancy in their means of generating control forces and moments. These aircraft have, as primary control surfaces, a single rudder and pairwise elevators and aileron/spoiler units that provide yaw, pitch, and roll moments with sufficient bandwidth to be used in stabilizing and maneuvering the airframe. Beyond this, throttling the engines can provide additional moments, but on a much slower time scale. Other aerodynamic surfaces, such as leading and trailing edge flaps, are only intended to be placed in a position and left, and are, hence, very slow-moving. Because of this, loss of a primary control surface strongly degrades the controllability of the vehicle, particularly when the failed effector becomes stuck in a non-neutral position where it exerts a disturbance moment that must be countered by the remaining operating effectors.

The second challenge in recovering safe flight is that these vehicles are not agile, nor can they tolerate large accelerations. This is of special importance when, at the outset of the recovery maneuver, the aircraft is flying toward the ground, as is frequently the case when there are major control hardware failures.

Recovery of safe flight is examined in this paper in the context of trajectory optimization. For a particular transport aircraft, and a failure scenario inspired by an historical air disaster, recovery scenarios are calculated with and without control surface failures, to bring the aircraft to safe flight from the adverse flight condition that it had assumed, apparently as a result of contact with a vortex from a larger aircraft's wake. An effort has been made to represent relevant airframe dynamics, acceleration limits, and actuator limits faithfully, since these contribute to the lack of agility and control power that plays an important role in defining what can be achieved with the vehicle when it is in extremis.

2 Vehicle Model

The aircraft model which is used in this study is adapted from a 6-degree-of-freedom simulation of Langley Research Center's now-retired 737-100 research aircraft, documented in [1,2]. The model assumes constant mass, rotating spherical Earth, and U.S. 1976 standard atmosphere [3] with no winds. The airframe dynamics are expressed in body axes, and vehicle attitude is propagated using quaternions.

The vehicle's control effectors are rudder, flaps, horizontal stabilizer, elevator, aileron/spoiler, and right and left engines. The aerodynamic and thrust forces are represented as tabular functions of these variables, along with aerodynamic angles and airspeed or Mach number and altitude. This gave roughly 90 data tables drawn from the original simulation software, where they were used with piecewise multilinear table lookups. In order to preserve differentiability in the optimization model, a piecewise linear-quartic scheme (which fits multi-quartic chamfers to the multilinear interpolant near tabulated points) was employed for table lookup. This software is documented in [4]. The simulation model additionally included dependencies on aerodynamic angle rates and load factor, but these were ignored because of their small contributions to the dynamical response.

The aerodynamic control surfaces are represented as integrators of control surface rate commands, subject to inequality constraints on position and rate. For example, the elevator position δ_E and rate σ_E are related by

$$\dot{\delta}_E = \sigma_E \quad (1)$$

subject to specified limits

$$-\bar{\sigma}_E \leq \sigma_E \leq \bar{\sigma}_E \quad \text{AND} \quad \delta_E^-(V) \leq \delta_E \leq \delta_E^+(V) \quad (2)$$

where the position limits are tabular functions of airspeed. This pattern holds true for all control surfaces except for

aileron/spoiler, whose position limits are tabular functions of altitude and Mach number, and the horizontal stabilizer, which has fixed mechanical limits. Each of the two engines is modelled separately. Thrust is a tabular function of engine pressure ratio, e , Mach and altitude; e itself satisfies

$$\dot{e} = \sigma_e, \quad \sigma_E = \begin{cases} 0.3 & e_c \geq e + 0.3 \\ e_c - e & \text{ELSE} \\ -0.54 & e_c \leq e - 0.54 \end{cases} \quad (3)$$

where e_c is the commanded value of e .

Thus far, the ailerons and spoilers have been referred to as a single unit. This is because, on the study aircraft, hardware linkages couple their motion. In particular, the right spoiler deflection is related to aileron deflection δ_A by

$$\delta_{S_R} = \max \left\{ 0, \frac{32}{15} \delta_A - \frac{8}{3} \right\} \quad (4)$$

where δ_A and δ_{S_R} are expressed in degrees. The left spoiler mirrors this, deflecting when the aileron deflection is negative. This relationship is not differentiable and, so, should confidently be expected to cause difficulty in optimization computations which require a guarantee of adequate smoothness for convergence. The aileron/spoiler linkage is modelled smoothly by driving the spoiler deflections from the aileron rate command σ_A , modified by a squashing function on δ_A . Again, for the right spoiler,

$$\dot{\delta}_{S_R} = \frac{32}{15} \sigma_A \frac{1}{1 + \exp\{25 - 20\delta_A\}} \quad (5)$$

It should be noted that the vehicle model from [1,2] included a number of logical branches in which calculated quantities changed discretely as vehicle states passed thresholds. These were carried into the optimization model, but smoothed using appropriately defined squashing functions.

3 Trajectory Optimization Formulation

In September 1994, a Boeing 737-300 aircraft, USAir Flight 427, crashed on approach to Pittsburgh after encountering the vortex wake field of a passing 727 aircraft. Results from a simulation study of this 737, reconstructed from the recovered flight data, indicated that the crash may have been due to adverse yaw moments caused by a stuck rudder [5]. This specific aircraft incident was selected as the testcase for the work reported in this paper. It should be noted that the USAir 427 aircraft was a 737-300, rather than the uniquely short-bodied Langley 737-100 used in this study. The ‘‘300’’ is larger all around, with more powerful engines. Because

we are studying the Flight 427 scenario, but applying it to a different transport aircraft, the results are of qualitative applicability to the Flight 427 situation.

Table 1 lists the vehicle state used as an initial condition for the study trajectories. Those quantities marked with an \times in the left column were taken from [5] at the point in time where their simulation indicated that Flight 427’s rudder became stuck at 17.6 degrees of deflection. The engine pressure ratio values, e_R and e_L , were not available in [5], but could be approximated from the data in the NTSB Accident Report for this incident [6]. The other displayed quantities were fit to the dynamics of the study aircraft.

Table 1. USAir 427 adverse flight conditions.

\times	Altitude	5500 ft
\times	Total velocity	315 ft/sec
	X-body velocity	306.22 ft/sec
	Y-body velocity	54.15 ft/sec
	Z-body velocity	-28.14 ft/sec
\times	Roll angle	-75 deg
\times	Pitch angle	-22 deg
\times	Yaw angle	25 deg
	Roll rate	-4.69 deg/sec
	Pitch rate	8.59 deg/sec
	Yaw rate	-12.60 deg/sec
\times	Vertical acceleration	2.0 g
\times	Longitudinal acceleration	-0.35 g
	e_L, e_R	1.64

These quantities were imposed as initial conditions on the trajectories discussed in the next section. Not shown are control surface initial conditions that were defined as a result of the acceleration terms in Table 1.

The trajectory optimization results in the following section were obtained by approximating the solution of the plant equations by collocation, using a midpoint Euler discretization formula that provides 2^{nd} -order accuracy, with equally spaced integration intervals. The optimization computations were carried out using the SNOPT 5.3 [7] nonlinear programming code. Gradients of dynamics and constraints were supplied to SNOPT analytically, and were obtained by applying the ADIFOR 2.1 [8] FORTRAN differentiation package to the source code that defines the plant model, constraints, and cost function. The organization of the various elements of this trajectory optimization problem, including discretization, constraints, boundary conditions, cost function, ADIFOR-generated gradients, and the call to SNOPT is managed by MADS4.3 [9], a FORTRAN 90/77 code developed at Langley Research Center.

The key performance issue in recovery of safe flight is to recover while losing as little altitude as possible – in order to avoid ground contact – and without violating airframe and crew safety acceleration placards. This certainly makes

selection of the cost function simple; i.e. maximize terminal altitude. Since the aircraft is initially traveling downward, a nonpositive altitude rate

$$\dot{h} \leq 0 \quad (6)$$

is imposed throughout the trajectory, in order to assure a meaningful solution. After the solution is obtained, it is verified that (6) is never an active constraint on the solution. The acceleration placards constraining the recovery trajectories are given in Table 2.

Z-body acceleration	+/- 2g
Y-body acceleration	+/- 1.5g
Y-body acceleration rate	+/- 2g/sec

Having defined cost function, initial conditions, and placard constraints, there remains termination of the recovery maneuver. Because of the degraded controllability of an aircraft with control effector failures, it may be difficult or impossible to bring the aircraft to a steady trim condition; furthermore, even if trimmed flight is possible, it may occur after the minimum altitude in the recovery trajectory has passed. Therefore, the terminal condition for these trajectories was selected as

$$\left. \begin{array}{l} \dot{h} = 0 \\ \dot{V} \geq 0 \\ \psi\dot{\psi} \leq 0 \\ \theta\dot{\theta} \leq 0 \\ \phi\dot{\phi} \leq 0 \end{array} \right\} \quad (7)$$

where ψ , θ , and ϕ are the euler angles. In other words, the aircraft has stopped descending, and has a non-negative energy rate. If the airframe is rotating, it is rotating back to a centered position. This appears to ensure that the aircraft can be flown from the terminal point of the recovery maneuver without losing more altitude.

4 Upset Recovery

In this section, two main scenari are considered. First, recovery from the initial conditions of Table 1 with minimum altitude loss is calculated with a healthy set of control effectors, to serve as an ideal baseline against which to consider the case of the rudder hardover suggested by [5]. In analyzing the “healthy” case we, in fact, consider two subscenari – recovery with the ailerons and spoilers linked using (5), and again, allowing the spoilers to operate independently of the ailerons. This was done because, at the time of writing, the authors are still wrestling with the problem of obtaining

a solution for the stuck rudder case in which the ailerons and spoilers are linked, and which satisfies the placards in Table 2. This difficulty highlights the importance of losing a control effector in an aircraft with negligible control redundancy.

Figures 1-9 display features of the recovery trajectories for the no-failure cases, computed using 40 integration intervals. The solid lines correspond to independent spoilers and the dash-dotted lines to coupled aileron/spoilers. The dashed lines, on the control surface histories, are their position limits. The maneuver is short in duration, lasting less than 5 seconds, and loses roughly 400 feet in altitude. It is also somewhat extreme, as can be seen from the acceleration and euler angle plots. Unsurprisingly, allowing the spoilers to move independently enhances the performance; in this case, by roughly 6%. Note that, the flaps are aggressively used, decreasing \dot{V} and enhancing lift. This turns out to be very important to recovering the vehicle. We have not been successful in computing a no-failure recovery maneuver that satisfied acceleration placards with realistically coupled aileron/spoiler, without using flaps. Interestingly, it looks as though the pilot could simply turn them on, then off at the outset of the maneuver, freeing his or her hands to wrestle with the yoke and throttles. This may, on examination of further upset scenari, generalize to a trainable pilot action for recovering control.

Figures 10-19 display corresponding data for recovery (with independent spoilers) for the same initial conditions, but including a rudder hardover failure. Two trajectories are presented. The optimized trajectory for maximizing altitude resulted in undesirable responses in the accelerations (Figures 14 and 15). In order to determine the importance of these extraneous-looking temporal features, the trajectory was recalculated, adding a integral penalty on the sum of the squared control surface rates, scaled by 10^{-2} . This was seen to have a fairly negligible effect on performance. In the Figures, the dash-dotted lines depict response without the control rate penalty and the solid lines are the response with it. Additionally, obeying the trajectory optimization rule of thumb that it is easier to solve a problem where the plant can meet the constraints easily than one where it can not, the object of the optimization problem was inverted from maximizing final altitude for a fixed rudder deflection to maximizing constant rudder deflection for a fixed final altitude. This permitted variation of the rudder setting during the iterations, and dramatically eased the solution process. For an altitude loss of 4190 ft, the maximized rudder deflection without the control rate penalty was 17.61 deg., and with it was 17.54 deg.; both of which correspond well to 17.6 deg at which the data in Table 1 were drawn.

The Figures show a trajectory that is startlingly different from the no-fail case on several counts. First, the trajectory duration is an order of magnitude larger. As can be seen from Figure 10, after the initial altitude loss, there is

a leg where altitude is almost unchanged for the rest of the trajectory. This occurs shortly after 20 sec, and the change can be seen in the euler angle histories, as the aircraft laboriously brings itself to a sustainable attitude. Although the aircraft speed is slowing down during the latter portion of the maneuver, the terminal \dot{V} value is slightly positive, thus satisfying the terminal energy rate condition. During the whole of the maneuver, the vehicle wallows, with oscillating normal and side accelerations of smaller magnitude than was seen in the no-fail case, consistent with the reduced availability of control authority. It is interesting to note that there is almost no use of the flaps in this case. Instead, the independence of the spoilers is exploited, bringing them both up early on in the trajectory to accomplish the braking function.

5 Conclusions

Recovery of safe flight for a particular aircraft, in a specific initial adverse condition has been examined, with and without a specific control failure. It was seen that under optimal circumstances, the adverse vehicle state could be corrected with little altitude loss. In addition, a control failure which proved fatal in practice was corrected, assuming independently acting spoilers. Generalizing these results to a comprehensive set of upset scenari will be time consuming, but could offer valuable heuristic piloting insights.

6 References

1. *TCV/User Oriented FORTRAN Program for the B737 Six DOF Dynamic Model*, Sperry Systems Management, Report No. SP-710-021, March 1981.
2. Goodwin, A.E., *NASA 515 Flight Control System Description RSFS Aircraft*, Boeing Commercial Airplane Co., Report No. D6-34279, Vol. 1-2, Sept. 1976.
3. *U.S. Standard Atmosphere, 1976*, NOAA, NASA, USAF, Oct. 1976.
4. Moerder, D.D. *Linear-Quartic Chamfer Splines for Efficient Smooth Modelling of Tabular Data*, NASA TM to be published.
5. Parks, E.K., et. al., "Reconstruction of the 1994 Pittsburgh Airplane Accident Using a Computer Simulation", *AIAA Journal of Aircraft*, Vol. 35, No. 5, Sept. - Oct. 1998, pp. 665-670.
6. *Uncontrolled Descent and Collision with Terrain, USAIR Flight 427, Boeing 737-300, N513AU Near Aliquippa, Pennsylvania, September 8, 1994*, National Transportation Safety Board, NTSB/AAR-99/01, Mar. 1999.

7. Gill, P.E., et. al., *User's Guide for SNOPT 5.3: A FORTRAN Package for Large-Scale Nonlinear Programming*, May 20, 1998.
8. Bischof, C., et. al., *ADIFOR 2.0 Users' Guide (Revision D)*, Mathematical, Information, and Computational Sciences Division, U.S. Department of Energy, Technical Memorandum No. 192, June 1998.
9. Moerder, D.D. and Khong, T.H., *MADS 4.3 Users' Guide*, November 2000, Draft Report - to be published.

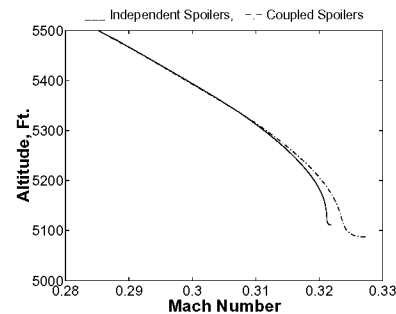


Figure 1: No Failure Mach Number vs. Altitude.

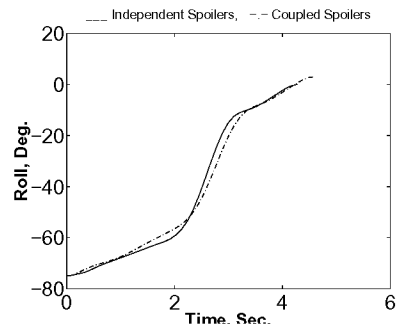


Figure 2: No Failure Roll Angle.

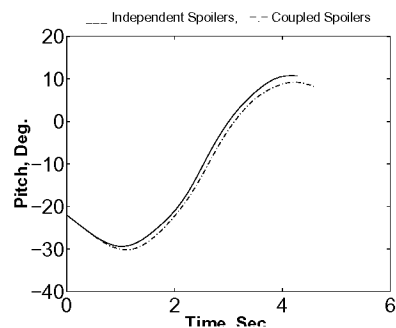


Figure 3: No Failure Pitch Angle.



Figure 4: No Failure Yaw Angle.



Figure 5: No Failure Normal Acceleration.



Figure 6: No Failure Side Acceleration.

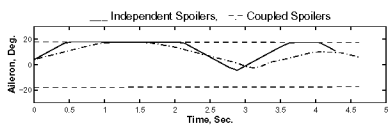


Figure 7: No Failure Aileron.



Figure 8: No Failure Right Spoiler.

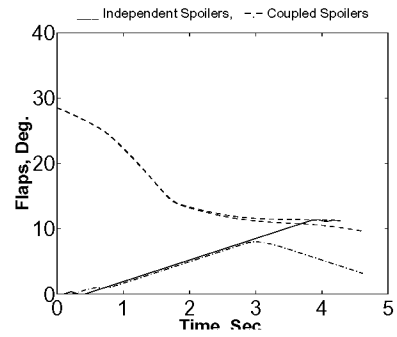


Figure 9: No Failure Flaps.

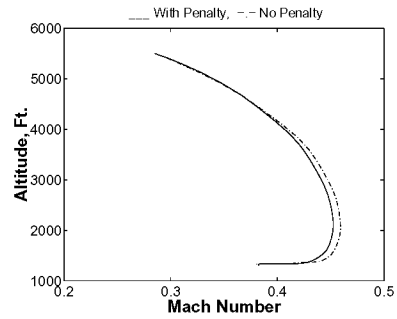


Figure 10: Stuck Rudder Altitude vs. Mach.

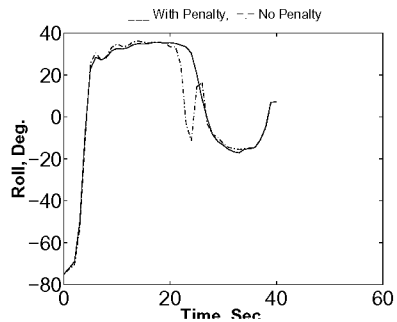


Figure 11: Stuck Rudder Roll Angle.

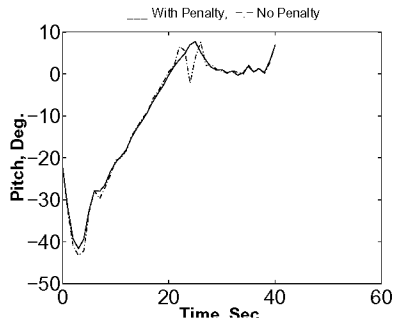


Figure 12: Stuck Rudder Pitch Angle.

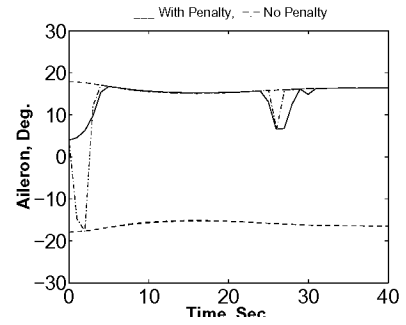


Figure 16: Stuck Rudder Aileron.

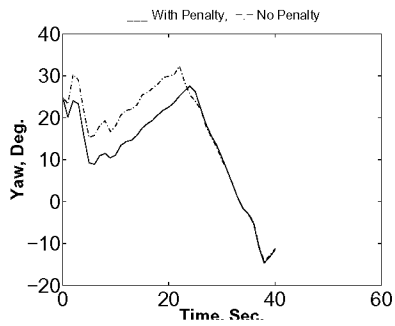


Figure 13: Stuck Rudder Yaw Angle.

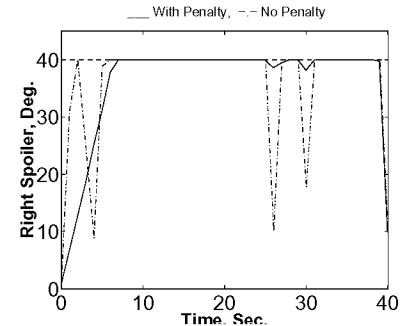


Figure 17: Stuck Rudder Right Spoiler.

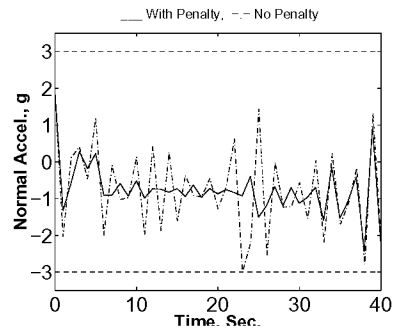


Figure 14: Stuck Rudder Normal Acceleration.

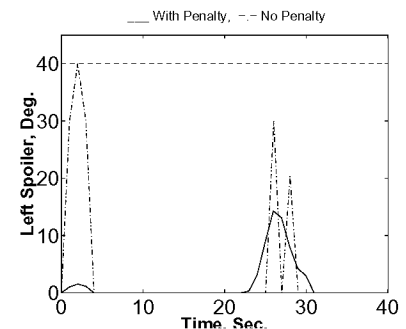


Figure 18: Stuck Rudder Left Spoiler.

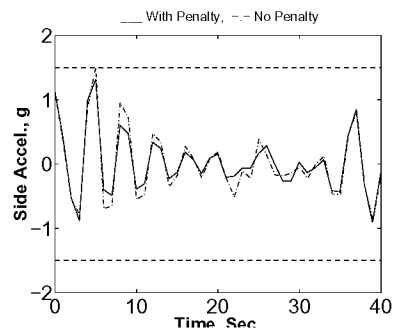


Figure 15: Stuck Rudder Side Acceleration.

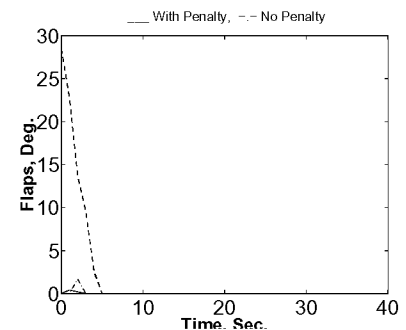


Figure 19: Stuck Rudder Flaps.